ACS Catalysis

Research Article

pubs.acs.org/acscatalysis

Aminolactone Chiral Modifiers for Heterogeneous Asymmetric Hydrogenation: Corrected Structure of Pantoyl-Naphthylethylamine, In-Situ Hydrogenolysis, and Scanning Tunneling Microscopy Observation of Supramolecular Aminolactone/Substrate Assemblies on Pt(111)

Guillaume Goubert, Vincent Demers-Carpentier, Richard P. Loach, Raphaël Lafleur-Lambert, Jean-Christian Lemay, John Boukouvalas,* and Peter H. McBreen*

Department of Chemistry and C3V, Université Laval, Québec, Canada G1V 0A6

Supporting Information

ABSTRACT: As established by Baiker and co-workers, pantoyl-naphthylethylamine (PNEA) is an efficient synthetic chiral modifier for the asymmetric hydrogenation of ketopantolactone (KPL) to pantolactone on supported Pt catalysts. We report a scanning tunneling microscopy (STM) study of PNEA and PNEA-derived aminolactone species on Pt(111) and a reassignment of the relative stereochemistry of the modifier. Robust organic chemistry methods were used to establish that the structure of PNEA is *R,S* rather than *R,R*. The dissociative chemisorption of a fraction of PNEA adsorbed on Pt(111) yields two fragments that we attribute to a process involving C−N bond scission. We show that C−N bond scission occurs under hydrogenation conditions on PNEA-modified Pt/Al_2O_3 catalysts, forming the aminolactone amino-4,4-dimethyldihydrofuran-2-one (AF). STM measurements on (*S*)-AF and 2,2,2-trifluoroacetophenone coadsorbed on Pt(111) show the formation of isolated 1:1 complexes. In contrast, measurements on coadsorbed (*S*)-AF and KPL show fluxional supramolecular AF/KPL assemblies. The possibility that such assemblies contribute to the overall enantioselectivity observed for PNEA-modified Pt catalysts is discussed.

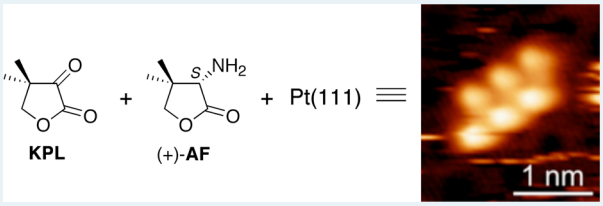

KEYWORDS: *heterogeneous asymmetric hydrogenation, scanning tunneling microscopy, chiral aminolactones, chemisorbed diastereomeric complexes, stereostructure reassignment, pantoylnaphthylethylamine, ketopantolactone, Orito reaction*

INTRODUCTION

The heterogeneous asymmetric hydrogenation of carbonyl compounds on a chirally modified Pt surface (Orito reaction)[1,2] is an inherently green process with potential applications in the production of pharmaceuticals and a host of other fine chemicals. Although significant progress has been made, only a handful of activated ketones are suitable substrates for the Orito reaction, thereby severely limiting its practical use. Expanding the substrate scope necessitates a better understanding of the origin of asymmetric induction and, ultimately, the development of custom-designed chiral modifiers that rival the naturally occurring cinchona alkaloids originally used by Orito.[1] The latter goal has proved to be especially elusive.[3]

Of the numerous alternative modifiers screened over the past two decades only a few can be categorized as promising or effective.[3] A notable example is pantoylnaphthylethylamine (PNEA), synthesized by Baiker and co-workers in a comprehensive study of a library of modifiers derived from (*R*)-1-(1-naphthyl)ethylamine, (*R*)-NEA.[4a] Hydrogenation of ketopantolactone[4] or 1,1,1-trifluoro-2,4-pentanedione[5] on PNEA-modified platinum afforded enantioselectivities competitive with those obtained with the best cinchona alkaloids. Importantly, the intact stereochemistry of PNEA was crucial because its C2-epimer (*epi*-PNEA) was not nearly as effective in the enantioselective hydrogenation of ketopantolactone (KPL).[4b] In the specific case of the enantioselective hydrogenation of KPL, a difference of 34% in ee, 74% versus 40%, was found between the two epimers.[4b] The respective identities of PNEA and *epi*-PNEA were deduced as **2** and **1** (Figure 1) on the basis of NOE−NMR experiments and theoretical calculations.[4b] The anticipated superior conformational rigidity of **2** over **1** was proposed to play a decisive role in achieving high enantioselectivity.[4b] Our studies, reported herein, demonstrate that the structures of PNEA and *epi*-PNEA should be revised to **1** and **2**, respectively (Figure 1).

Enantioselective hydrogenation on chirally modified metals is intimately dependent on both chemisorption interactions and chemisorption-modulated intermolecular interactions.[6] The results of surface studies, when placed in the context of the relevant catalysis literature, are of great value in understanding aspects of enantioselective reactions on metal catalysts.[6−9] In the surface science component of this study, we use scanning

Received: August 30, 2013
Revised: October 7, 2013
Published: October 9, 2013

   dx.doi.org/10.1021/cs4007588 | *ACS Catal.* 2013, 3, 2677−2683

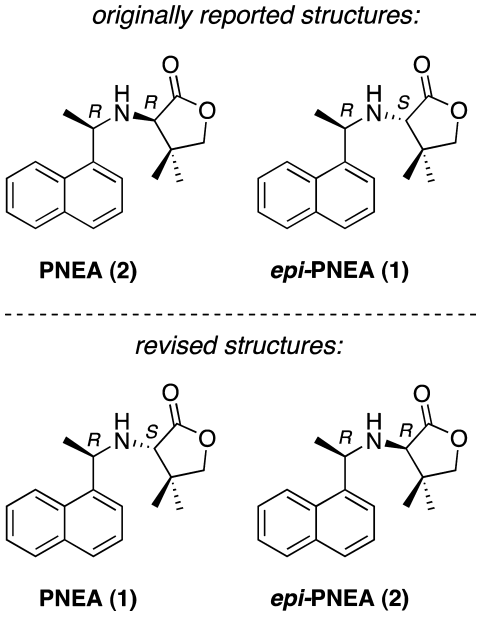

Figure 1. Originally reported[4a,b] and revised structures of PNEA and its epimer.

tunneling microscopy (STM) to explore the chemisorption of **1** and (*S*)-amino-4,4-dimethyldihydrofuran-2-one, (+)-AF, (Scheme 1B) and their complexation with prochiral substrates

Scheme 1. Synthesis and Transformation of PNEA to Lactones (+)-AF and (+)-Boc-AF

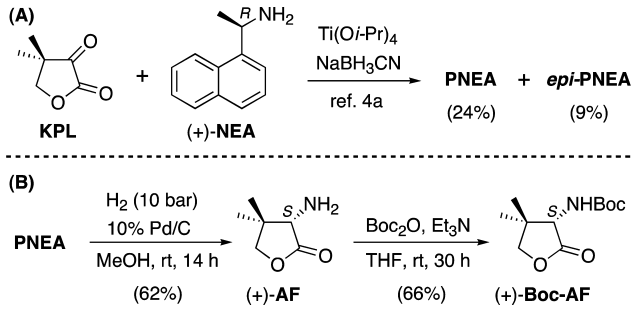

on Pt(111). Measurements on (*S*)-AF are included because we find that it is formed under hydrogenation conditions using PNEA-modified Pt/Al_2O_3.

It is interesting to compare the structure of AF with that of 1-(1-naphthyl)ethylamine (NEA), PNEA, or protonated cinchonidine. Although all four molecules contain an amino hydrogen-bond donor group located close to a chiral center, only NEA, PNEA, and cinchonidine contain an aromatic group. It is widely accepted that the extended aromatic groups of these modifiers serve the key role of anchoring them to the metal surface.[2] In this way, an optimal surface coverage of isolated chiral sites can be maintained during the course of a reaction. This, in turn, enables the modifiers to form 1:1 complexes with the generally more mobile substrate molecules. Because AF does not possess a strong anchoring group it is a priori not expected to compete for surface sites in the presence of PNEA. However, the STM data presented herein for (*S*)-AF coadsorbed with KPL suggest a mechanism whereby (*S*)-AF might coadsorb with PNEA under reaction conditions, creating an additional chiral environment on the surface.

RESULTS AND DISCUSSION

The relative stereochemistry of PNEA was studied using robust organic chemistry methods. Following the procedure of Baiker,[4a] reductive amination of KPL with (*R*)-NEA afforded PNEA and *epi*-PNEA in yields of 24 and 9% after flash chromatography (Scheme 1A). Their ^1H and ^{13}C NMR spectra, order of elution, and optical data were in good agreement with those of the major and minor diastereoisomers described in the literature.[4a] The stereochemistry of the major isomer (PNEA) was determined by hydrogenolysis[10] to (+)-AF and ensuing conversion to (+)-Boc-AF (Scheme 1B). Because the (*S*)-configuration of the latter had previously been secured by stereoselective synthesis,[11] it follows that the absolute stereochemistry of the newly formed asymmetric center of PNEA is *S*, and that of *epi*-PNEA should be *R*. Furthermore, we were able to obtain good crystals of *epi*-PNEA, thereby confirming its relative stereochemistry as depicted in **2** by X-ray diffraction analysis (Figure 2). These findings unambiguously establish the

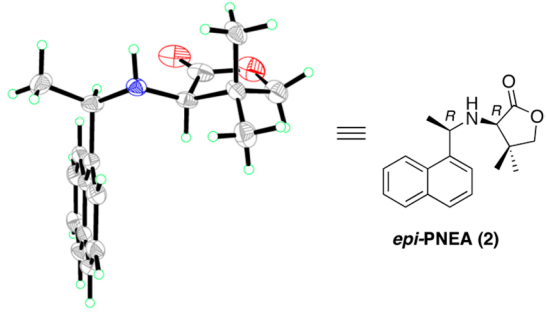

Figure 2. X-ray structure of *epi*-PNEA (**2**).

correct stereostructures of PNEA and *epi*-PNEA as **1** and **2**, respectively. As such, they should have obvious implications in future efforts directed toward uncovering the precise molecular events responsible for chirality transfer from PNEA in the hydrogenation of KPL.

The chemisorption of PNEA on Pt(111) was studied using scanning tunneling microscopy imaging as part of an exploration of chirality transfer processes on chirally modified platinum. The images A–D shown in Figure 3 are attributed to molecularly adsorbed PNEA. Their shape and contrast resemble those previously interpreted for (*R*)-NEA on Pt(111),[7] but with the addition of an extra protrusion. The observation of several distinct images for PNEA (Figure 3A–

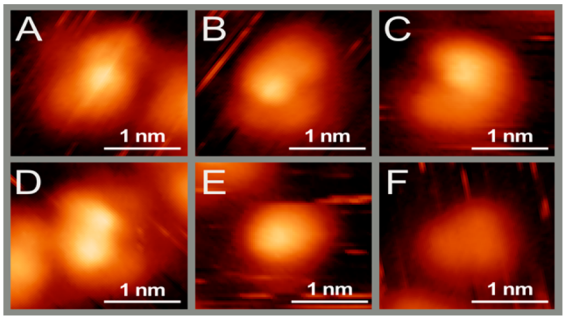

Figure 3. STM images for PNEA adsorbed on Pt(111) at room temperature. (A–D) Images attributed to adsorbed conformers of PNEA; (E, F) Images attributed to two adsorbed dissociation fragments. Imaging conditions: bias, 1–1.1 V; current, 0.3–0.4 nA.

dx.doi.org/10.1021/cs4007588 | *ACS Catal.* 2013, 3, 2677–2683

D) is attributed to the coexistence of surface conformers that differ in the orientation of the naphthyl and lactone groups relative to the ethylamine moiety. We assign the contributions of the naphthyl, ethylamine and lactone moieties to the PNEA images by comparison with the previously established relationship between the adsorption geometries and STM images of (*R*)-NEA/Pt(111). For example, the PNEA image shown in Figure 3B is schematically deconstructed into three parts in Figure 4. The combination of the parts denoted 2 and 3

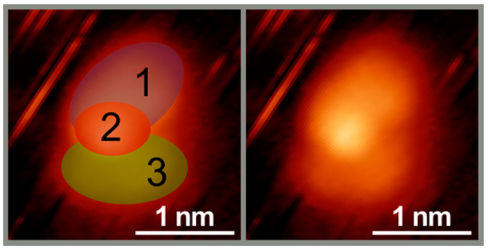

Figure 4. Proposed attribution of the protrusions in the STM image of PNEA/Pt(111) shown in Figure 3 B: (1) lactone moiety, (2) ethylamine moiety, (3) naphthyl moiety.

resembles images of (*R*)-NEA, in which a bright protrusion locates the ethylamine group and a dimmer oval protrusion locates the naphthyl group. The extra protrusion, denoted 1, is then attributed to the lactone moiety of PNEA. No change from one type of image to another was observed during the room temperature STM experiments.

In addition to the features attributed to PNEA, there are two smaller motifs in the STM images (Figure 3E, F). These motifs account for roughly 7% of all imaged species. The STM image 3F matches our previously reported images for vinylnaphthalene formed by the partial dehydrogenation of ethyl naphthalene on Pt(111).[12] As illustrated in Scheme 2B,

Scheme 2. (A) Proposed C−N Bond Scission in a Small Fraction of PNEA Adsorbed on Pt(111) in Ultrahigh Vacuum at Room Temperature To Form Aminolactone- And Ethylnaphthyl-Related Chemisorbed Fragments. (B) Proposed Dehydrogenation of the Ethylnaphthyl Fragment To Yield Adsorbed Vinylnaphthalene[a]

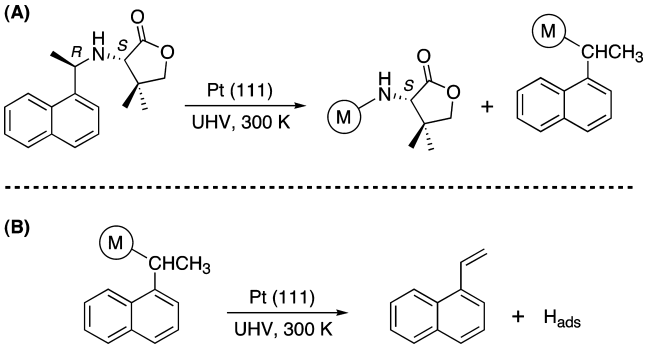

[a]M represents a Pt(111) surface site.

vinylnaphthalene could result from scission of a C−N bond in adsorbed PNEA, followed by the expected[12,13] partial dehydrogenation of the alkyl substitutent to yield adsorbed vinylnapthalene. The accompanying adsorbed fragment formed by CN bond scission would then be an aminolactone species (Scheme 2A).

To test this hypothesis, a search for aminolactone formation under reaction conditions using PNEA-modified Pt/Al_2O_3 was carried out. Our tests show that formation of (*S*)-amino-4,4-dimethyldihydrofuran-2-one, (*S*)-AF, occurs in acetic acid at 10 bar H_2. The formation of AF is thus consistent with the partial decomposition (Scheme 2A) of PNEA on Pt(111) that is suggested by the STM data. It also reveals that at least one additional chiral agent is present under reaction conditions using PNEA-modified Pt catalysts in protic solvents. We find that AF formation occurs in acetic acid and in a mixture of toluene and trifluoroacetic acid (TFA), but only in trace amounts in toluene. Interestingly, Baiker and co-workers found that the performance of PNEA as a chiral modifier in the enantioselective hydrogenation of KPL to pantolactone also depends strongly on the solvent used.[4a] They found enantiomeric excesses of 74% in acetic acid, 5% in toluene, and 79% in a mixture of toluene and trifluoroacetic acid (20 equiv of TFA with respect to PNEA).

To study its chemisorption properties, we prepared (*S*)-AF using the procedure shown in Scheme 1B. STM data for (*S*)-AF on Pt(111) are presented in Figure 5. Two distinct types of

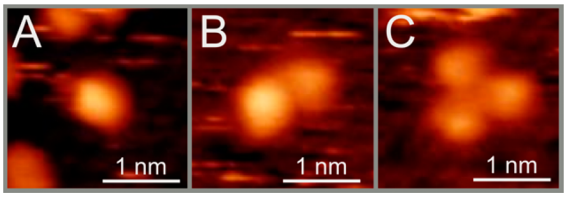

Figure 5. STM images obtained following (*S*)-AF adsorption on Pt(111) at room temperature: (A) monomer, (B) dimer, (C) trimer.

motifs are observed, one bright and one dim. Isolated (*S*)-AF images are, with few exceptions, of the bright type (Figure 5A). Dimers are formed by one bright and one dim motif (Figure 5B). Although most trimers (Figure 5 C) contain only dim motifs, reversible interconversion between dim and bright motifs is observed for individual molecules in trimers. The fraction of trimers observed increases with increasing coverage. The contrast within images of individual molecules in trimers is not strong but is sufficient to show that trimers are themselves chiral structures, as can be seen from Figure 5C. In the absence of spectroscopic or DFT studies of the adsorption geometry, we speculate that (*S*)-AF undergoes both N−Pt lone pair bonding and an interaction of the carbonyl group with the surface. For example, the amine group of (*R*)-NEA on Pt(111) forms an on-top bond to a Pt atom,[6,7] NH_3 bonds on-top on Pt(111),[14] and Medlin et al.[15] have reported that the adsorption of γ-butyrolactone on Pt(111) occurs through its oxygenate functionality. Two adsorption geometries in which (*S*)-AF combines N−Pt and carbonyl-Pt bonding are proposed in Scheme 3. The structures are related by a 180° rotation around the C*−N bond while keeping the N−Pt bond fixed. In one geometry (Scheme 3B), the hydrogen at the chiral center points away from the surface, and in the second geometry (Scheme 3A), it points toward the surface. We speculate that repulsive interactions between the dimethyl groups in (*S*)-AF dimers can be minimized by pairing structures such as A and B and that both dimers and trimers form closed structures in which every carbonyl and amine group forms an NH···OC interaction.

Given that (*S*)-AF can form under hydrogenation conditions using PNEA-modified Pt, we investigated the coadsorption of

dx.doi.org/10.1021/cs4007588 | ACS Catal. 2013, 3, 2677−2683

Scheme 3. Two proposed adsorption geometries for (*S*)-AF. The hydrogen on the chiral carbon is indicated in green. In structure (A) it is hidden behind the chiral carbon

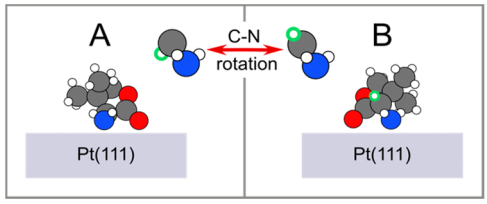

(*S*)-AF and KPL on Pt(111). Because it is difficult to reliably distinguish between images of the two adsorbates, we associate KPL/(*S*)-AF complexation with the formation of structures not observed for (*S*)-AF alone. KPL alone does not form multimolecular structures on Pt(111) at the temperatures studied, and (*S*)-AF alone forms the dimer and trimer structures shown in Figure 5. Examples of supramolecular structures formed only when both (*S*)-AF and KPL are present on the surface are shown in Figure 6. The smaller structures

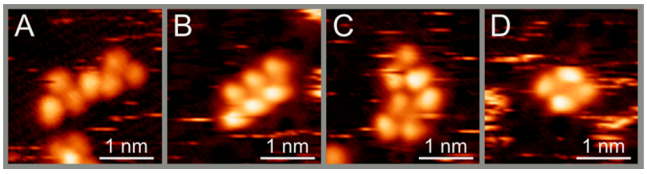

Figure 6. STM images of supramolecular assemblies formed by the coadsorption of (*S*)-AF and KPL on Pt(111) at room temperature.

contain four molecules (Figure 6D), but bigger assemblies also form (Figures 6A–C). As shown in Figure 7, some similar

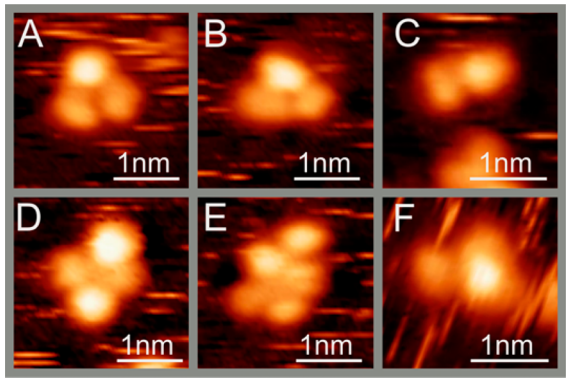

Figure 7. Selected assemblies formed through the coadsorption of KPL and PNEA on Pt(111) at room temperature. The assemblies shown in A–E are attributed to the interaction of KPL and aminolactone species resulting from the dissociative chemisorption of a fraction of chemisorbed PNEA. Complex F is attributed to the interaction of a PNEA molecule with one KPL.

assemblies are observed for the interaction of KPL with the PNEA dissociation fragment that we attribute to an aminolactone species (Figure 3E, Scheme 2A). However, for low coverages of PNEA, only small structures are found, including some 1:1 KPL/fragment and $(KPL)_2$/fragment complexes (Figure 7A–C) that are not seen in (*S*)-AF/KPL coadsorption experiments. When the coverage of PNEA is increased, quadrimer complexes (Figure 7D) and bigger ones (Figure 7E) are observed. The latter structures closely resemble those formed by (*S*)-AF/KPL (Figure 6C, D), suggesting that the aminolactone fragment on Pt(111) can undergo hydrogenation to AF under the ultrahigh vacuum conditions of the experiment.

The larger assemblies formed by (*S*)-AF and KPL are fluxional, displaying changes in shape and in the total number of molecules, but existing in one form or another over long times at localized regions of the surface. A representative example of this behavior is shown in Figure 8. Thus, it appears that (*S*)-AF's main mode of interaction with KPL is not through 1:1 complexation, but through the formation of multimolecular $((S)\text{-AF})_n/(KPL)_m$ structures. This can be explained by the high surface mobility of both (*S*)-AF and KPL and by the presence of both hydrogen bond acceptor and donor functions in (*S*)-AF, enabling the formation of a variety of relatively stable networks. In contrast, when 2,2,2-trifluoroacetophenone (TFAP) and (*S*)-AF are coadsorbed on Pt(111), we observe the formation of only 1:1 complexes. Assuming that complexation always involves NH···O bonding, these images (Figure 9) can be used to probe stereodirection of

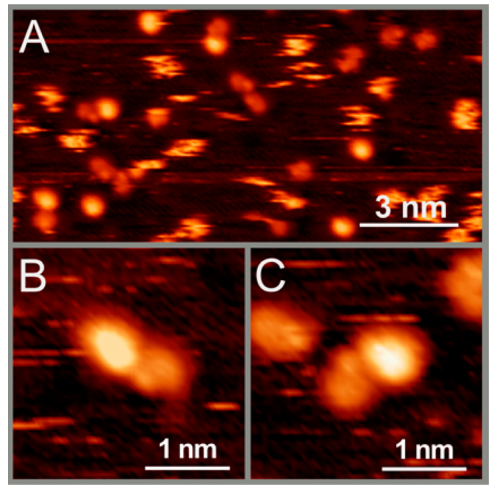

Figure 9. STM images of complexes formed by coadsorbed (*S*)-AF and TFAP on Pt(111) at room temperature: (A) Large scan image, (B–C) (*S*)-AF/TFAP complexes.

TFAP by (*S*)-AL.[7] A visual inspection of 390 (*S*)-AF/TFAP complexes reveals that bright (*S*)-AF forms 87% of the observed complexes. The prochiral ratio (pro-*R*/pro-*S* ratio)

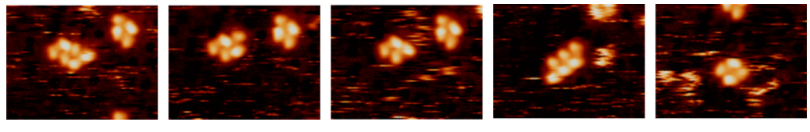

Figure 8. Time-lapsed images (0, 80, 160, 240, 520 s) of supramolecular assemblies of KPL and (*S*)-AF in a single area (6.8 by 5.1 nm^2) of the Pt(111) surface. The measurements were performed at room temperature.

dx.doi.org/10.1021/cs4007588 | *ACS Catal.* 2013, 3, 2677–2683

for TFAP in these complexes is 3.6. For complexes involving dark (*S*)-AF, the prochiral ratio is 1.6.

It remains to be established if AF can function as an effective Orito reaction modifier despite the fact that it does not possess an aromatic anchoring group. As an individual molecule, the fact that it is not strongly adsorbed would act against AF being an effective modifier. A more strongly adsorbing molecule, for example, TFAP, might out-compete it for surface sites, with the result that the number of chiral sites on the surface would become vanishingly low. Such a situation was demonstrated in elegant work by Lambert and co-workers for proline and isophorone on Pd catalysts.[16] They found that the prochiral substrate, isophorone, was adsorbed on the catalyst surface to the exclusion of the chiral auxiliary, proline. Bartok and co-workers have also published interesting observations on competitive adsorption occurring in binary mixtures of substrates.[17] In the case of KPL, multimolecular $((S)\text{-AF})_n/(\text{KPL})_m$ structures, possessing an appreciable adsorption energy, might enable the continual replenishment of chiral sites on the surface through the symbiotic interaction between AF and KPL. The multimolecular assemblies observed for AF/KPL are intermediate between the 1:1 or 1:2 complexes observed for (*R*)-NEA/methyl-3,3,3 trifluoropyruvate[6] and (*R*)-NEA/TFAP,[7] for example, and the ordered systems created by coadsorption of methylacetoacetate and tartaric acid or glutamic acid on Ni(111).[18] As discovered by Baddeley and co-workers,[18] the latter two systems demonstrate that the disordered and mobile adsorbed modifier can transform into ordered mixed prochiral molecule/chiral molecule domains on adsorption of methylacetoacetate. In the present case, AF and KPL form transient local superstructures rather than extended domains. We speculate that multimolecular structures might enable (*S*)-AF formed in situ from PNEA to coadsorb with PNEA on the metal catalyst and, thus, contribute to the observed ee in the hydrogenation of KPL.

CONCLUSIONS

Organic chemistry methods show that the correct stereostructure of the Orito reaction synthetic chiral modifier PNEA is *R,S*. This information is important in any attempt to understand the mechanism for chirality transfer from PNEA, because PNEA and *epi*-PNEA display significantly different ee's for hydrogenation of KPL on Pt catalysts. STM measurements suggest that PNEA on Pt(111) can undergo partial decomposition via C−N bond scission at room temperature. Similarly, reactor studies show that C−N bond scission to form (*S*)-AF occurs under hydrogenation conditions on PNEA-modified Pt. The STM study of the complexation of (*S*)-AF with TFAP and KPL on Pt(111) reveals that TFAP and (*S*)-AF form isolated complexes in which a TFAP binds to a single (*S*)-AF while KPL and (*S*)-AF form a variety of multimolecular structures. Some of the larger (*S*)-AF/KPL structures combine fluxionality with relatively good stability in that assemblies are located in the same local area of the surface over long periods. It is not yet possible to determine if these superstructures alter the prochiral ratio of KPL on the surface. We are currently exploring if AF can function as a chiral modifier for the enantioselective hydrogenation of KPL on Pt.

EXPERIMENTAL SECTION

The STM experiments were carried out in an ultrahigh vacuum (UHV) chamber equipped with a SPECS Aarhus STM-150 microscope. All images were acquired at room temperature at a constant tunneling current in the 0.3−0.6 nA range and a bias voltage in the 0.8−1.1 V range. WSxM image treatment software (www.nanotec.es)[19] was used to adjust brightness and contrast. The Pt(111) crystal (MaTecK Gmbh) was cleaned by cycles of Ar^+ ion bombardment at 600 K and oxygen treatment at 900 K, followed by flash annealing to 1050 K. TFAP (99% purity), KPL (97% % purity), and (*R*)-NEA (99% purity) were purchased from Sigma-Aldrich and further purified by pumping and freeze−thaw cycles in the gas handling vacuum line prior to introduction into the vacuum chamber.

Synthesis of PNEA and *epi*-PNEA. According to the literature procedure,[4a] (*R*)-NEA (1.29 mL, 8 mmol) and KPL (1.28 g, 10 mmol) were dissolved in titanium(IV) isopropoxide (4 mL), and the viscous mixture was stirred at rt under argon. After 20 min, this became a more homogeneous yellow solution. After 4 h, $NaBH_3CN$ (340 mg, 5.4 mmol) and EtOH (12 mL) were added. The reaction was stirred overnight. Then again, $NaBH_3CN$ (340 mg, 5.4 mmol) and 3−4 few drops of acetic acid were added. The following day, the reaction was quenched with water, and the resulting precipitate was filtered over Celite and washed with ethanol. The filtrate was concentrated in vacuum, dissolved in ethyl acetate, and filtered over Celite again. The filtrate was concentrated, and the crude mixture was purified by flash chromatography (7% ethyl acetate/hexanes) over silica using a Teledyne Combiflash R_f system. The two diastereomers PNEA and *epi*-PNEA eluted in that order and were isolated in 24% and 9% yield, respectively. PNEA was a viscous colorless oil that eventually solidified after significant drying, and *epi*-PNEA formed as an off-white solid that was recrystallized in ether/pentane to provide white rhombic crystals for X-ray diffraction studies.

*Data for PNEA (**1**, Revised Structure).* R_f = 0.38 (7% EtOAc/hexanes); mp: 48−50 °C; $[\alpha]_D^{20}$ = −35.5° (*c* 1.25, $CHCl_3$). IR (NaCl, film): 3336, 3049, 2964, 2895, 1770, 1463, 1141, 1010, 780 cm^{-1}. ^1H NMR (400 MHz, $CDCl_3$): δ 1.04 (s, 3H), 1.11 (s, 3H), 1.51 (d, *J* = 6.8 Hz, 3H), 1.57 (s, 2H), 2.16 (br s, 1H), 3.23 (br s, 1H), 3.71 (d, *J* = 8.8 Hz, 1H), 3.89 (d, *J* = 8.8 Hz, 1H), 4.88 (q, *J* = 7.9 Hz, 1H), 7.47−7.56 (m, 3H), 7.64 (d, *J* = 6.1 Hz, 1H), 7.77 (d, *J* = 6.1 Hz, 1H), 7.88 (d, *J* = 6.0 Hz, 1H), 8.14 (d, *J* = 6.1 Hz, 1H). ^{13}C NMR (100 MHz, $CDCl_3$): δ 177.9, 140.0, 134.0, 131.4, 129.0, 127.5, 126.1, 125.7, 125.5, 122.6, 122.4, 76.4, 63.3, 51.8, 41.0, 23.9, 23.8, 20.1. ESI-HRMS: *m/z* for $C_{18}H_{21}NO_2$: $[M + H]^+$ calcd, 284.1645; found, 284.1644.

*Data for epi-PNEA (**2**, Revised Structure).* R_f = 0.35 (7% EtOAc/hexanes); mp: 56−57.5 °C; $[\alpha]_D^{20}$ = +171.1° (*c* 1.26, $CHCl_3$). IR (NaCl, film): 3336, 3049, 2964, 2896, 1770, 1463, 1141, 1011, 780 cm^{-1}. ^1H NMR (400 MHz, $CDCl_3$): δ 1.04 (s, 3H), 1.11 (s, 3H), 1.51 (d, *J* = 6.8 Hz, 3H), 1.57 (s, 2H), 2.16 (br s, 1H), 3.23 (br s, 1H), 3.71 (d, *J* = 8.8 Hz, 1H), 3.89 (d, *J* = 8.8 Hz, 1H), 4.88 (q, *J* = 7.9 Hz, 1H), 7.47−7.56 (m, 3H), 7.64 (d, *J* = 6.1 Hz, 1H), 7.77 (d, *J* = 6.1 Hz, 1H), 7.88 (d, *J* = 6.0 Hz, 1H), 8.14 (d, *J* = 6.1 Hz, 1H). ^{13}C NMR (100 MHz, $CDCl_3$): δ 179.4, 140.6, 134.2, 131.8, 129.1, 127.8, 126.1, 125.7, 125.7, 124.3, 123.5, 76.9, 64.4, 52.7, 40.6, 24.8, 23.1, 20.0. ESI-HRMS: *m/z* for $C_{18}H_{21}NO_2$: $[M + H]^+$ calcd, 284.1645; found, 284.1639.

Synthesis of (*S*)-(+)-Aminolactone (AF). PNEA (**1**, 123 mg) was dissolved in 5 mL of methanol in a high-pressure reaction flask, 32 mg of palladium on carbon (10%) was added, and the mixture was stirred under 10 bar hydrogen pressure for 14 h. The mixture was then filtered over Celite, washed with

dx.doi.org/10.1021/cs4007588 | ACS Catal. 2013, 3, 2677−2683

dichloromethane, and evaporated down to a yellow residue. This was purified by flash column chromatography over silica gel (CH_2Cl_2/MeOH/NH_4OH, 40:1:0.1) to furnish (*S*)-aminolactone (AF) as a white solid (50.8 mg, 91% yield). R_f = 0.34 (10% MeOH/CH_2Cl_2); mp: 61 °C; $[\alpha]_D^{20}$ = +4.96° (*c* 0.88, $CHCl_3$), +16.8° (*c* 0.91, MeOH). IR (NaCl, film): 3388 (br), 3329 (br), 2963, 2897, 1779, 1465, 1118, 1008 cm^{-1}. ^1H NMR (400 MHz, $CDCl_3$): δ 3.95 (d, *J* = 8.8 Hz, 1H), 3.85 (d, *J* = 8.8 Hz, 1H), 3.28 (s, 1H), 1.48 (br s, 2H), 1.14 (s, 3H), 0.96 (s, 3H). ^{13}C NMR (100 MHz, $CDCl_3$): δ 178.6, 76.7, 60.2, 40.3, 23.0, 18.9. ESI-HRMS: *m*/*z* for $C_6H_{11}NO_2$ $[M+H]^+$ calcd, 130.0863; found, 284.1644.

Synthesis of (*S*)-(+)-*N*-Boc-aminolactone (Boc-AF). (*S*)-Aminolactone (AF, 25.0 mg) was dissolved in 1.5 mL of anhydrous THF, along with 18.2 mg of di-*tert*-butyl carbonate (1.2 equiv) and 40 μL of triethylamine. After overnight stirring at rt, the reaction mixture was concentrated in vacuo and partioned between ethyl acetate and aqueous saturated sodium bicarbonate. The combined organic layers were washed with 5% aqueous potassium hydrogen sulfate, and brine; dried over sodium sulfate; and concentrated in vacuo to give a white solid. Flash column chromatography on silica gel (20% ethyl acetate/hexanes) furnished 29.3 mg of (*S*)-*N*-Boc-aminolactone (Boc-AF) as a white powder (66%). mp: 141−142 °C (lit.:[11] 138−140 °C); $[\alpha]_D^{20}$ = +53.7° (*c* 0.87, $CHCl_3$). Lit.:[11] $[\alpha]_D$ = +63° (*c* 1, $CHCl_3$). IR (NaCl, film): 3310 (br), 3280, 2983, 2925, 2853, 1779, 1701, 1678, 1550, 1367, 1142 cm^{-1}. ^1H NMR (400 MHz, $CDCl_3$): δ 0.99 (s, 3H), 1.23 (s, 3H), 1.46 (s, 9H), 3.98−4.03 (m, 2H), 4.36 (d, *J* = 7.6 Hz, 1H), 4.85 (br s, 1H). ^{13}C NMR (100 MHz, $CDCl_3$): δ 175.3, 155.8, 80.5, 76.7, 59.6, 41.1, 28.2, 23.3, 19.8. ESI-HRMS: *m*/*z* for $C_{11}H_{19}NO_4$ $[M + H]^+$ calcd, 230.1387; found, 230.1360.

Formation of (*S*)-AF under Hydrogenation Conditions Using PNEA-Modified Pt/Al_2O_3. The 5 wt % Pt−Al_2O_3 catalyst (Sigma Aldrich) was pretreated at 400 °C in flowing nitrogen for 1 h, then 1 h with 10% hydrogen in argon and cooled to room temperature under flowing nitrogen for 2 h. The hydrogenation was carried out in a Teflon-lined Berghof BR-25 reactor. The reaction mixture was magnetically stirred at 250 rpm. The products were analyzed by ^1H and ^{13}C NMR.

PNEA (**1**, 53.0 mg) was dissolved in 5 mL of acetic acid, 53.1 mg of catalyst was added, and the mixture was stirred under 10 bar hydrogen pressure for 24 h. The mixture was then filtered over Celite, washed with dichloromethane; the solvent was quenched with aqueous saturated $NaHCO_3$; and the organic layer was extracted and dried with sodium sulfate, filtered, and concentrated in vacuo. The resulting yellow oil was purified by flash column chromatography over silica gel (CH_2Cl_2/MeOH/NH_4OH, 40:1:0.1) to give (*S*)-amino-4,4-dimethyldihydrofuran-2-one (7.6 mg, 31% yield). $[\alpha]_D^{20}$ = +17.7° (*c* 0.32, MeOH), whose ^1H and ^{13}C NMR spectra were identical to those described above.

■ ASSOCIATED CONTENT

Supporting Information

NMR and XRD data. This material is available free of charge via the Internet at http://pubs.acs.org.

■ AUTHOR INFORMATION

Corresponding Author

*E-mails: john.boukouvalas@chm.ulaval.ca; peter.mcbreen@chm.ulaval.ca.

Notes

The authors declare no competing financial interest.

■ ACKNOWLEDGMENTS

The work was supported by NSERC, FQRNT, and the CFI grants. The work was carried out within the FQRNT-funded Center on Catalysis and Green Chemistry (CCVC). G.G., R.L.-L., and J.-C.L. acknowledge FQRNT graduate student scholarships. V.D.-C. and R.P.L. acknowledge NSERC graduate student scholarships.

■ REFERENCES

(1) (a) Orito, Y.; Imai, S.; Niwa, S. *J. Chem. Soc. Jpn.* **1979**, 1118−1120. (b) Orito, Y.; Imai, S.; Niwa, S. *J. Chem. Soc. Jpn.* **1980**, 670−672.

(2) (a) Vargas, A.; Mondelli, C.; Baiker, A. In *Catalytic Methods in Asymmetric Synthesis: Advanced Materials, Techniques, and Applications*; Gruttadauria, M., Giacalone, F., Eds.; John Wiley & Sons: New York, 2011, pp 291−322. (b) Mallat, T.; Orglmeister, E.; Baiker, A. *Chem. Rev.* **2007**, *107*, 4863−4890. (c) Margitfalvi, J. L.; Talas, E. *Catalysis* **2010**, *22*, 144−278. (d) Bartók, M. *Curr. Org. Chem.* **2006**, *10*, 1533−1567. (e) Blaser, H.-U.; Studer, M. *Acc. Chem. Res.* **2007**, *40*, 1348−1356. (f) Murzin, D. Y.; Mäki-Arvela, P.; Salmi, T. *Cat. Rev: Sci. Eng.* **2005**, *47*, 175−256.

(3) Tálas, E.; Margitfalvi, J. L. *Chirality* **2010**, *22*, 3−15.

(4) (a) Orglmeister, E.; Mallat, T.; Baiker, A. *Adv. Synth. Catal.* **2005**, *347*, 78−86. (b) Orglmeister, E.; Bürgi, T.; Mallat, T.; Baiker, A. *J. Catal.* **2005**, *232*, 137−142. (c) Balazs, L.; Mallat, T.; Baiker, A. *J. Catal.* **2005**, *233*, 327−332.

(5) (a) Diezi, S.; Hess, M.; Orglmeister, E.; Mallat, T.; Baiker, A. *Catal. Lett.* **2005**, *102*, 121−125. (b) Diezi, S.; Ferri, D.; Vargas, A.; Mallat, T.; Baiker, A. *J. Am. Chem. Soc.* **2006**, *128*, 4048−4057. (c) Diezi, S.; Hess, M.; Orglmeister, E.; Mallat, T.; Baiker, A. *J. Mol. Catal. A: Chem.* **2005**, *239*, 49−56.

(6) (a) Demers-Carpentier, V.; Rasmussen, A. M. H.; Goubert, G.; Ferrighi, L.; Dong, Y.; Lemay, J.-C.; Masini, F.; Zeng, Y.; Hammer, B.; McBreen, P. H. *J. Am. Chem. Soc.* **2013**, *135*, 9999−10002. (b) Lavoie, S.; Mahieu, G.; McBreen, P. H. *Angew. Chem., Int. Ed.* **2006**, *45*, 7404−7407.

(7) Demers-Carpentier, V.; Goubert, G.; Masini, F.; Lafleur-Lambert, R.; Dong, Y.; Lavoie, S.; Mahieu, G.; Boukouvalas, J.; Gao, H.; Rasmussen, A. M. H.; Ferrighi, L.; Pan, Y.; Hammer, B.; McBreen, P. H. *Science* **2011**, *334*, 776−780.

(8) (a) Kyriakou, G.; Beaumont, S. K.; Lambert, R. M. *Langmuir* **2011**, *27*, 9687−9695. (b) Baddeley, C. J.; Jones, T. E.; Trant, A. G.; Wilson, K. E. *Top. Catal.* **2011**, *54*, 1348−1356. (c) Bonello, J. M.; Williams, F. J.; Lambert, R. M. *J. Am. Chem. Soc.* **2003**, *125*, 2723−2729. (d) Burkholder, L.; Garvey, M.; Weinert, M.; Tysoe, W. T. *J. Phys. Chem. C* **2011**, *115*, 8790−8797. (e) Boscoboinik, J. A.; Bai, Y.; Burkholder, L.; Tysoe, W. T. *J. Phys. Chem. C* **2011**, *115*, 16488−16494. (f) Raval, R. *Chem. Soc. Rev.* **2009**, *38*, 707−721.

(9) (a) Rees, N. V.; Taylor, R. J.; Jiang, Y.-X.; Morgan, I. R.; Knight, D. W.; Attard, G. W. *J. Phys. Chem. C* **2011**, *115*, 1163−1170. (b) Gordon, A. D.; Zaera, F. *Angew Chem. Int. Ed.* **2013**, *52*, 3453−3456. (c) Meemken, F.; Maeda, N.; Hungerbühler, K.; Baiker, A. *Angew. Chem., Int. Ed.* **2012**, *51*, 8212−8216. (d) Goubert, G.; McBreen, P. H. *ChemCatChem* **2013**, *5*, 683−685.

(10) Nugent, T.; Marinova, S. M. *Synthesis* **2013**, *45*, 153−166.

(11) Freskos, J. N. *Synth. Commun.* **1994**, *24*, 557−563.

(12) Goubert, G.; Demers-Carpentier, V.; Masini, F.; Dong, Y.; Lemay, J. C.; McBreen, P. H. *Chem. Commun.* **2011**, *47*, 9113−9115.

(13) Ranke, W.; Weiss, W. *Surf. Sci.* **2000**, *465*, 317−330.

(14) (a) Liang, Z.; Kim, H.; Kim, Y.; Trenary, M. *J. Phys. Chem. Lett.* **2013**, *4*, 2900−2905. (b) Ford, D. C.; Xu, Y.; Mavrikakis, M. *Surf. Sci.* **2005**, *587*, 159−174.

(15) Horiuchi, C. M.; Medlin, J. W. *Surf. Sci.* **2010**, *604*, 98−105.

(16) (a) McIntosh, A. L.; Watson, D. J.; Lambert, R. M. *Langmuir* **2007**, *23*, 6113−6118. (b) McIntosh, A. L.; Watson, D. J.; Burton, J. W.; Lambert, R. M. *J. Am. Chem. Soc.* **2006**, *128*, 7329−7334.
(17) (a) Balázsik, K.; Szőri, K.; Szőllősi, G.; Bartók, M. *Catal. Commun.* **2011**, *12*, 1410−1414. (b) Balázsik, K.; Szőri, K.; Szőllősi, G.; Bartók, M. *Chem. Commun.* **2011**, *47*, 1551−1552.
(18) Trant, A. G.; Baddeley, C. J. *J. Phys. Chem. C* **2011**, *115*, 1025−1030.
(19) Horcas, I.; Fernández, R.; Gómez-Rodríguez, J. M.; Colchero, J.; Gómez-Herrero, J.; Baro, A. M. *Rev. Sci. Instrum.* **2007**, *78*, 013705.